International Journal of Multidisciplinary and Current Research ISSN: 2321-3124
Research Article Available at: http://ijmcr.com

Quasiparticle-phonon description of ^{103}Mo isotope

O. Jdair[1], Z.Housni[1], J. Inchaouh[1], M. K. Jammari[2], A. Khouaja[1], M. Ferricha-Alami[1], H. Chakir[1], M.L.Bouhssa[1], S.Boudhaim[1], N.Harakat[1], M.Fiak[1], M. Krim[1] and A.Kartouni[1]

[1]Department of Physics, LPMC-ERSA, Faculty of Sciences Ben M'Sik Hassan II Casablanca University, Casablanca, Morocco B.P. 5366
[2]Department of Physics, LPN , Faculty of Sciences Ain chock, Hassan II Casablanca University, Casablanca, Morocco B.P. 5366

Accepted 02 May 2017, Available online 06 May 2017, **Vol.5 (May/June 2017 issue)**

Abstract

The evolution of the ground-state nuclear shapes in describing low-lying states of ^{103}Mo isotope, is studied within the quasiparticle-phonon coupling plus rotor. Calculations based on the deformed mean field of Nilsson, the monopole-pairing interaction (BCS) and the quadrupole-quadrupole force. Microscopic structure of quadrupole phonon is given from the Tamm-Dancoff Approximation (TDA). The two effects of the recoil and Coriolis forces are included with the hypothesis of a symmetric rotational motion. The nuclear deformation and shape coexistence inherent to this mass region are shown to play a relevant role in the understanding of the spectroscopic features of the ground and low-lying one-quasineutron states.

Keywords: *Neutron-rich nuclei; quasiparticle states; low-lying levels; γ-phonon.*

1. Introduction

The nuclear structure of neutron-rich nuclei near A ~ 100 is of particular interest in studying the effect of nuclear deformation and shape coexistence phenomena of transitional region. For the even $_{38}$Sr and $_{40}$Zr isotopes a sudden onset of strong deformation is observed from N = 60, whereas the lighter isotopes up to N=58 are rather spherical. There were showed for N=59 isotones, using the quasiparticle-Rotor-Model, that some shapes coexist, particularly the two unique-parity states $\pi g_{9/2}$ and $\nu h_{11/2}$, in the structure of ^{97}Sr, ^{99}Zr and ^{96}Rb isotopes [1, 2]. The clear identification of the bandhead spins, their deformations and the Nilsson orbitals of N=59 isotones, has given a new insights in understanding the mechanisms responsible of this rapid change in shapes, which are highlighted from the quadrupole moment measurements of the ground state for Rubidium isotopes [3]. However, using the self-consistent Total Routhian Surface (TRS) model for N > 59 isotones, there have been found that the nuclear structure of ^{105}Mo and ^{103}Zr has a medium triaxiality parameter of γ = -19° and γ = 0° [4], respectively. The triaxial effect, sign of strong deformation, is more important for Mo isotopes than Zr ones, using RTRP and TRS models [4, 5]. Experimentally, producing Zr and Mo isotopes from ^{238}U(α,f) fusion-fission reaction mechanism, the analysis of experimental data performed in the framework of the particle–rotor-model showed that the triaxial degree of freedom is more important for Mo than Zr isotopes [6]. In these calculations, the Cranked shell model was used for the study of the crossing frequency of the aligned band. It was concluded that the alignment of $\nu h_{11/2}$ neutron orbital is responsible for the first band crossing in the even Zr and Mo isotopes [6], which has a great consequence on the behavior of $5/2^-(532)$ bands in the odd Zr and Mo isotopes. In the transitional region A~100, the nuclear shape is soft spherical-deformed, which is theoretically a reason to do not use a rigid triaxiality. It is then a better way to treat this spherical-deformed shape by using the coupling between (axial) rotation and vibration. Therefore, in our work, we have used a Soloviev [7] inspired model: Quasiparticle Phonon plus rotor**,** where TDA phonon was used instead of RPA one. We have developed a microscopic description for the low-lying excited states of odd-A = 105 and 130 nuclei [8-9]. For the transitional region, a microscopic structure is considered for the quadrupole phonon by means of Tamm-Dancoff Approximation (TDA), developed in the Ring-Schuk book [10]. This method is microscopic and provides two-quasiparticle structure of the quadrupole vibrational core (γ-phonon) in contrast to the phenomenological model in which the phonon structure is excluded**.**

This paper is then organized as follows where the theoretical formalism of total Hamiltonian is developed in section 2, with a discussion of the intrinsic eigenvalue problem. In section 3, the results of calculations are presented and discussed in the case of existing experimental data for ^{103}Mo [6]. And finally, our

conclusions for the nuclear structure in transitional region are presented in section 4.

2. Theoretical Procedures

The calculations presented in this paper are investigated via a new code based on Nilsson, BCS and TDA formalisms. The originality of our new method is based on the diagonalization of total Hamiltonian, emanating from individual and collective correlations.

Total Hamiltonian formalism

Theoretically, the odd-A nucleus is treated as a system of an extra-nucleon coupled to an even-even core, with the standard assumption of total Hamiltonian [11],

$$H = H_{rot} + H_{int} \quad (1)$$

Where H_{rot} is the collective kinetic energy associated to the rotation of the nucleus. And, H_{int} is the intrinsic motion treated as one-body deformed potential field H_{sp} plus a two-body residual interaction composed by a short range constant pairing force H_p and a quadrupole part H_Q of the long range multipole-multipole force [10].

The kinetic energy of rotational motion in the laboratory system is developed as:

$$H_{rot} = A_1 R_1^2 + A_2 R_2^2 + A_3 R_3^2 \quad (2)$$

where R_k is the component of the collective angular momentum along the axis of the intrinsic system. A_k is the corresponding rotational parameter defined as $A_k=\hbar^2/2\Im_k$ with the moment of inertia parameter $\Im_k$ around the three principal axis k=1,2,3 of the nuclear mass distribution.

In (2) we gave a general triaxial form. However, in this paper we limit our analysis to the case of a nucleon coupled to an axially symmetric rotor [12]. The rotational Hamiltonian can then be reduced to

$$H_{rot} = \hbar^2 (R_1^2 + R_2^2) /2\Im \quad (3)$$

with the same moment of inertia $\Im$ along the two axis k = 1, 2 perpendicular to the symmetry axis k=3.

The total angular momentum I is composed of two terms: the collective rotation of the core R and the angular momentum of the extra-nucleon J; I = R + J. Since I is a conserved quantity, R in (3) is replaced by I and J. The total Hamiltonian (1) is then expressed as [12]:

$$H = H_{int} + H_I + H_C \quad (4)$$

where

$$H_{int} = H_{sp} + H_P + H_Q + H_J$$
$$H_I = A_R(I^2 - I_3^2)$$
$$H_C = -A_R(I_+J_- + IJ_+)$$
$$H_J = A_R(J^2 - J_3^2) \quad (5)$$

with $I_\pm = I_1 \pm iI_2$, $J_\pm = J_1 \pm iJ_2$ and the rotational coefficient $A_R = \hbar^2/2\Im$.

The total Hamiltonian H is thus separated into three terms, the intrinsic H_{int}, rotational H_I and Coriolis H_C terms which couple the intrinsic and rotational motions. The intrinsic Hamiltonian is more interesting from a physical point of view. It is separated into four parts. The first, H_{sp}, contains the deformed potential field which governs the independent motion of nucleons. In this sense, we prefer to use the Nilsson harmonic oscillator model which is rather simple and is more performed to describe a deformed nucleus. Using second quantization, H_{sp} takes the simple form [13]

$$H_{sp} = \sum_{\nu\tau} e_{\nu\tau} a^+_{\nu\tau} a_{\nu\tau} \quad (6)$$

where $a^+_{\nu\tau}$ ($a_{\nu\tau}$) is the operator that creates (destroys) a particle of nucleon type τ (neutron or proton) in a Nilsson orbital and with an energy $e_{\nu\tau}$. The quantum number ν stands for the asymptotic quantum along numbers $[Nn_zl_z]$ with the projection Ω_ν of the particle angular mom entum along the symmetry axis. The term H_p describes the monopole pairing interaction with the strength parameter G_τ and is written as [11]:

$$H_p = -\sum_{\nu\mu\tau} G_\tau a^+_{\nu\tau} a^+_{-\nu\tau} a_{-\mu\tau} a_{\mu\tau} \quad (7)$$

The next term H_Q is the quadrupole-quadrupole force and is expressed by [10]

$$H_Q = -\frac{1}{2}\chi \sum_{\tau\tau'} \{Q^+_{22}(\tau) Q_{22}(\tau') + Q^+_{2-2}(\tau) Q_{2-2}(\tau')\} \quad (8)$$

where the quadrupole moment of mass with γ = ± 2 is given as one-body interaction

$$Q_{2\gamma}(\tau) = \sum_{\nu\tau\mu} \langle \nu\tau | r^2 Y_{2\gamma} | \mu\tau \rangle a^+_{\nu\tau} a_{\mu\tau} . \quad (9)$$

The last term in equation (5) is the recoil force H_J. In many earlier works H_J was neglected with the argument that it could be absorbed in the independent nucleon motion of the potential average field [11]. Here, we have chosen to treat it in the same way as a residual interaction into the intrinsic motion. By using second quantization, H_J can be expressed as

$$H_J = \frac{1}{2} A_R \sum_{\tau\tau'} (J_+(\tau) J_-(\tau') + J_-(\tau) J_+(\tau')) \quad (10)$$

where the one-body interaction of the intrinsic momentum $J_\pm$ is written as

$$J_{\pm}(\tau)=\sum_{\nu\mu}\langle\nu\tau|J_{\pm}|\mu\tau\rangle a^{+}_{\nu\tau}a_{\mu\tau} \tag{11}$$

The term H_I in equation (4) represents the kinetic energy in the rotational motion and produces energy differences between states in a rotational band. The inclusion of the Coriolis force H_C requires the matrix of the model Hamiltonian H to be constructed and diagonalized within the space of symmetrized functions [11].

$$\left|IMK_{\rho}\right\rangle=\sqrt{\frac{2I+1}{16\pi^{2}}}\left\{D^{I}_{MK}\left|K_{\rho}\right\rangle+(-)^{I+K}D^{I}_{M-K}\left|\overline{K_{\rho}}\right\rangle\right\} \tag{12}$$

Here ρ is the quantum number of a given intrinsic states with a projection K of the intrinsic angular momentum along the symmetry axis. $|K_\rho\rangle$ can be obtained by resolution of the secular problem

$$H_{\text{int}}\left|K_{\rho}\right\rangle=(H_{sp}+H_{P}+H_{Q}+H_{J})\left|K_{\rho}\right\rangle=E^{\text{int}}_{K_{\rho}}\left|K_{\rho}\right\rangle \tag{13}$$

As it is well known, D^{I}_{MK} is the rotational matrix and is an eigenfunction of I^2 and I^3 with respective eigenvalue I(I+1) and K. Thus, a diagonalization of H within the basis states, equation (12) requires essentially to determine the matrix element of the Coriolis term H_C [12]

$$\left\langle IMK'_{\rho}\left|H_{C}\right|IMK_{\rho}\right\rangle=-A_{\text{R}}\left\{(-)^{I+\frac{1}{2}}\left(I+\frac{1}{2}\right)\left\langle K'_{\rho}\left|J_{+}\right|\overline{K_{\rho}}\right\rangle\delta_{K,\frac{1}{2}}\delta_{K',\frac{1}{2}}+\sqrt{(I\mp K)(I\pm K+1)}\left\langle K'_{\rho}\left|J_{\pm}\right|K_{\rho}\right\rangle\delta_{K',K\pm1}\right\} \tag{14}$$

As we can see from the above equations, the solutions must be obtained in a two-step process. First, the intrinsic eigenvalue equation (13) when solved gives a set of intrinsic states $|K_\rho\rangle$ and intrinsic energies E_K^{int}. From these states, different rotational wave functions of the form given in (12) are constructed. Then in a second step, a diagonalization of the Coriolis term is performed.

Intrinsic Hamiltonian formalism

To discuss the different terms in the intrinsic eigenvalue (13) we must first look for a possible solution of the system. By neglecting H_J and H_Q we have a model which describes an independent nucleon motion in a Nilsson deformed potential and where is added the pairing correlations. The BCS approximation is adopted so as to transform the system to an independent quasiparticle motion. The long range interaction of quadrupole type H_Q is introduced so to account for the dynamical mode of deformation or the vibrational excitation. We work in the frame of Tamm-Dancoff approximation in order to make a microscopic structure description for the γ-phonon state. Our intrinsic Hamiltonian will contain also a residual part of the rotational motion by retaining the recoil force H_J which is independent in regard to the total angular momentum I. The BCS method is an approximate approach to treat pairing correlation by using the Bogoliubov-Valatin transformation which makes change from particle to quasiparticle operators [14]

$$a^{+}_{\sigma\nu\tau}=U_{\nu\tau}\,\alpha^{+}_{\sigma\nu\tau}+\sigma V_{\nu\tau}\alpha_{-\sigma\nu\tau} \tag{15}$$

Here the operator $\alpha_{\sigma\nu\tau}^{+}$($\alpha_{\sigma\nu\tau}$) creates (destroys) a quasiparticle in state $|\sigma\nu\tau\rangle$ with a σ-sign depending to time reversal symmetry and where the occupation (non-occupation) probability is expressed by $U_{\nu\tau}$ ($V_{\nu\tau}$) . The expression deduced from $H_{sp}+H_P$ is given by

$$H_{BCS}=T+\sum_{\sigma\nu\tau}E_{\nu\tau}\alpha^{+}_{\sigma\nu\tau}\alpha_{\sigma\nu\tau} \tag{16}$$

where T is the BCS ground state energy and $E_{\nu\tau}$ is the energy of single quasiparticle

$$E_{\nu\tau}=\sqrt{\left(e_{\nu\tau}-\lambda-G_{\tau}V^{2}_{\nu\tau}\right)^{2}+\Delta^{2}_{\tau}} \tag{17}$$

where λ is the Lagrange multiplicator and Δ_τ is the energy gap.

In the same way, the transformation (15) allows the expression of quadrupole (9) and intrinsic (11) moments to change into form of quasiparticle terms:

$$Q_{2\gamma}(\tau)=\sum_{\sigma\sigma'=\pm1,\nu\nu'}G^{\gamma,\tau}_{\sigma\nu\sigma'\nu'}\alpha^{+}_{\sigma\nu\tau}\alpha_{\sigma'\nu'\tau}-\frac{1}{2}\sum_{\sigma\sigma'=\pm1,\nu\nu'}\left(\sigma'F^{\gamma,\tau}_{\sigma\nu-\sigma'\nu'}\alpha^{+}_{\sigma\nu\tau}\alpha^{+}_{\sigma'\nu'\tau}+\sigma F^{\gamma,\tau}_{-\sigma\nu\sigma'\nu'}\alpha_{\sigma\nu\tau}\alpha_{\sigma'\nu'\tau}\right) \tag{18}$$

where:

$$G^{\gamma,\tau}_{\sigma\nu\sigma'\nu'}=\left(U_{\nu\tau}U_{\nu'\tau}-V_{\nu\tau}V_{\nu'\tau}\right)\left\langle\sigma\nu\tau\left|r^{2}Y_{2\gamma}\right|\sigma'\nu'\tau\right\rangle \tag{19}$$

$$F^{\gamma,\tau}_{\sigma\nu\sigma'\nu'}=\left(U_{\nu\tau}U_{\nu'\tau}+V_{\nu\tau}V_{\nu'\tau}\right)\left\langle\sigma\nu\tau\left|r^{2}Y_{2\gamma}\right|\sigma'\nu'\tau\right\rangle \tag{20}$$

and:

$$J_{\pm}(\tau)=\sum_{\sigma\sigma'=\pm1,\nu\nu'}M^{\pm,\tau}_{\sigma\nu\sigma'\nu'}\alpha^{+}_{\sigma\nu\tau}\alpha_{\sigma'\nu'\tau}-\frac{1}{2}\sum_{\sigma\sigma'=\pm1,\nu\nu'}\left(\sigma'N^{\pm,\tau}_{\sigma\nu-\sigma'\nu'}\alpha^{+}_{\sigma\nu\tau}\alpha^{+}_{\sigma'\nu'\tau}-\sigma N^{\pm,\tau}_{-\sigma\nu\sigma'\nu'}\alpha_{\sigma\nu\tau}\alpha_{\sigma'\nu'\tau}\right) \tag{21}$$

Here:

$$M^{\pm,\tau}_{\sigma\nu\sigma'\nu'}=\left(U_{\nu\tau}U_{\nu'\tau}+V_{\nu\tau}V_{\nu'\tau}\right)\left\langle\sigma\nu\tau\left|J_{\pm}\right|\sigma'\nu'\tau\right\rangle \tag{22}$$

$$N^{\pm,\tau}_{\sigma\nu\sigma'\nu'}=\left(U_{\nu\tau}U_{\nu'\tau}-V_{\nu\tau}V_{\nu'\tau}\right)\left\langle\sigma\nu\tau\left|J_{\pm}\right|\sigma'\nu'\tau\right\rangle. \tag{23}$$

By introducing these new expressions respectively in (8) and (10), the quadrupole and the recoil forces can be decomposed as in the form $H_{00}+H_{11}+H_{20}+H_{22}+H_{31}+H_{40}$ where the subscript refer to the number of quasiparticle creation and annihilation operators. In this form, we noted that both one-body and two-body interactions should be considered [10]. In the frame of Tamm-Dancoff Approximation the creation operator of γ-phonon is defined as:

$$A^{+}_{\gamma}=\frac{1}{2}\sum_{\nu\mu\tau}\left(X^{\tau}_{\gamma}\right)_{\nu\mu}\alpha^{+}_{\nu\tau}\alpha^{+}_{\mu\tau} \tag{24}$$

This expression permits a microscopic structure description for the quadrupole vibrational core (γ-phonon

state) by showing the X-amplitudes which are related to two-quasiparticle excitations.

Intrinsic eigenvalue for odd-A nuclei

The resolution of (13) for an odd-A nucleus is perfected by a diagonalization within a basis formed by one-quasiparticle states (1-qp) and quasiparticle-phonon coupling states (qp-ph$_\gamma$). If we retain only the terms that do not have a zero matrix element within the states of this basis, the intrinsic Hamiltonian is then reduced to

$$H_{int} = H_{BCS} + H_{11}^{Q} + H_{20}^{Q} + H_{22}^{Q} + H_{31}^{Q} + H_{11}^{J} + H_{20}^{J} + H_{22}^{J} + H_{31}^{J} + H_{22}^{'P} \quad (25)$$

The Q and J terms are related respectively to quadrupole and recoil forces. The last term is H'$_{22}^{P}$ is a residual pairing interaction which was neglected in BCS approximation. The interaction between two-1qp states and qp-Ph$_\gamma$ states are given respectively by L_{11} and L_{22} matrix elements and that between 1-qp and qp-ph$_\gamma$ states by L_{31}. They are written as follows.

$$L_{11} = \langle BCS | \alpha_{K'\tau} (H_{BCS} + H_{11}^{Q} + H_{11}^{J}) \alpha_{K\tau}^{+} | BCS \rangle \quad (26)$$

$$L_{22} = \langle BCS | A_{\gamma'} \alpha_{K'\tau} (H_{BCS} + H_{11}^{Q} + H_{11}^{J} + H_{22}^{Q} + H_{22}^{J} + H_{22}^{'p}) \alpha_{K\tau}^{+} A_{\gamma}^{+} | BCS \rangle \quad (27)$$

$$L_{31} = \langle BCS | A_{\gamma} \alpha_{K'\tau} (H_{20}^{Q} + H_{20}^{J} + H_{31}^{Q} + H_{31}^{J}) \alpha_{K\tau}^{+} | BCS \rangle \quad (28)$$

The eigenvalue problem is written in matrix form

$$\begin{pmatrix} L_{11} & L_{31} \\ L_{31} & L_{22} \end{pmatrix} \begin{pmatrix} C_K^{\rho} \\ D_{K\gamma}^{\rho} \end{pmatrix} = E_{K_\rho}^{intr} \begin{pmatrix} C_K^{\rho} \\ D_{K\gamma}^{\rho} \end{pmatrix} \quad (29)$$

Where C_K^{ρ} represents the 1-qp component and $D_{K\gamma}^{\rho}$ the qp-ph$_\gamma$ component. The intrinsic eigenvalue E_K^{int} corresponds to the eigenvector

$$|K\rangle = \left(\sum_{\nu} C_{\nu}^{\rho} \delta_{K\Omega_\nu} \alpha_{\nu\tau}^{+} + \sum_{\nu\gamma} D_{\nu\gamma}^{\rho} \delta_{K=\Omega_\nu+\gamma} \alpha_{\nu\tau}^{+} A_{\gamma}^{+} \right) | BCS \rangle \quad (30)$$

The overlap between the 1-qp and qp-ph$_\gamma$ states is always zero. However, the overlap between two different qp-ph$_\gamma$ states can be non-zero so as they can form a non-orthogonal basis set

$$\begin{aligned} S_{ij} &= \langle i | j \rangle = \langle BCS | A_{\gamma'} \alpha_i \alpha_j^{+} A_{\gamma}^{+} | BCS \rangle \\ &= S_{ij} \delta_{\gamma'\gamma} - \sum_{\lambda} (X_{\gamma'})_{j\lambda} (X_{\gamma})_{i\lambda} \end{aligned} \quad (31)$$

where |i> is the qp-ph$_\gamma$ states. To solve this rather eigenvalue problem we adopt the method where we first solve the eigenvalue equation for the S_{ij} overlap matrix

$$\sum_j S_{ij} \omega_j^h = n_h \omega_i^h \quad (32)$$

The eigenvectors obtained can be written in the basis {|i>} as:

$$|\tilde{i}\rangle = \frac{1}{\sqrt{n_h}} \sum_i \omega_i^h |i\rangle \quad (33)$$

They have the property of being mutually orthogonal; they have a norm equal to unity and form a complete set. The amplitude D_ν^{ρ} in (30) are then calculated from the g-amplitudes in the following way

$$D_\nu^{\rho} = \sum_h \frac{1}{\sqrt{n_h}} g_h^{\rho} \omega_\nu^h \quad (34)$$

3. Results and discussion

The new code discussed in this work is developed for the transitional region A~100 with particular investigation of the low-lying states of ^{103}Mo, which are treated as a system of even-even core plus an extra nucleon. We have developed this code in respect to the following steps: Nilsson, BCS and TDA calculations. For the case of Nilsson calculation, we have reproduced the even-even core structure using conjointly the deformation parameter ε_2 from Möller data [15] and from Meyer data [16], the Kappa = 0.068 and Mu = 0.35 parameters of deformed average Nilsson field. The BCS pairing was fixed for proton and neutron by the well-known phenomenological relation $\Delta_p=\Delta_n=12/A^{1/2}$ [17]. And, for TDA calculation, the parameter of quadrupole force χ was fitted from the experimental energy of quadrupole vibrational core using the experimental from Guessous et al and Hua et al [6,18], where ^{102}Mo have E(2$^+$) =295 keV. We have summarised the effect of all parameters cited above in a subroutine diagonalizing the total Hamiltonian where the inertia parameters are determined semi-empirically using the energy of first excited state ($\varepsilon_2^2 \approx 1176(A^{7/3}E(2^+))^{-1}$) [19, 20]. The partial diagram provided by Nilsson is presented in figure 1 for the region of 50 ≤ N ≤ 82, where the level energy is a function of deformation parameter (ε_2) and the pairing correlation $G_p=19.6A^{-1}$ and G_n= (19.6-15.7(N-Z)A^{-1}) A^{-1} are obtained phenomenologicaly [21].

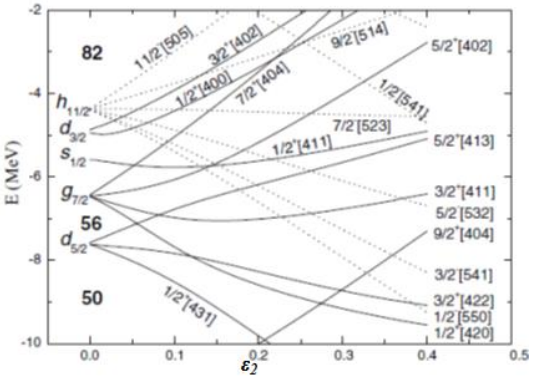

Fig.1: The Nilsson diagram of single particle levels for neutrons (50≤N≤82) as a function of deformation ε_2

For the ^{103}Mo, where the ^{102}Mo core is localised with a deformation parameter ε_2 = 0.3, we have to primarily identifying the ground state from the excited ones in a region where the excitation gap is more important regarding to the deformation parameter. We introduced the BCS method in which the correlation probability between quasiparticle operators (creation and annihilation) is well determined. With this method, we treat numerically for ^{103}Mo the energy of 10 up and down band-head levels – candidates to be the ground state - around the Fermi level. In table 1, with a precision of 10^{-7} after 7 iterations, we present for each subsequent level the calculated eigen-energy and their occupancy (U) and vacancy (V) probabilities.

Table 1: Quasiparticle energy levels calculated for ^{102}Mo (neutrons case) around the Fermi surface

Band-head number	Band-head levels	Energy-levels (MeV)	U	V
21	$5/2^+[422]$	5.959	0.100	0.995
22	$5/2^-[303]$	4.772	0.125	0.992
23	$1/2^-[301]$	4.749	0.126	0.992
24	$1/2^+[431]$	4.367	0.137	0.990
25	$7/2^+[413]$	3.814	0.158	0.987
26	$1/2^+[420]$	2.429	0.252	0.967
27	$1/2^-[550]$	2.043	0.305	0.952
28	$3/2^+[422]$	2.013	0.310	0.950
29	$9/2^+[404]$	1.559	0.419	0.907
30	$3/2^-[541]$	1.385	0.493	0.870
	Fermi level			
31	$3/2^+[411]$	1.342	0.856	0.517
32	$5/2^-[532]$	1.514	0.900	0.436
33	$5/2^+[413]$	1.865	0.941	0.338
34	$1/2^+[411]$	2.579	0.971	0.237
35	$7/2^-[523]$	3.159	0.981	0.191
36	$1/2^-[541]$	3.634	0.986	0.166
37	$5/2^+[402]$	3.855	0.988	0.156
38	$7/2^+[404]$	4.741	0.992	0.126
39	$1/2^-[530]$	5.231	0.993	0.114
40	$9/2^-[514]$	5.382	0.992	0.111

So, when looking for the closest energy level to the Fermi one, we could have a confusing decision if one treats and finds out the ground state only according to its energy level. In table 2, we carried out the whole possible ground and excited states correlated from particular states presented in table 1.

Table 2: BCS eigen-values for Nilsson orbitals of ^{102}Mo

<v/	<v'/	E(v) + E(v')
$5/2^+[422]$	$7/2^+[413]$	9.774
$5/2^+[422]$	$3/2^+[422]$	7.972
$5/2^+[422]$	$3/2^+[411]$	7.301
$5/2^+[422]$	$7/2^+[404]$	10.701
$5/2^-[303]$	$3/2^-[541]$	6.157
$-1/2^-[301]$	$1/2^-[301]$	9.498
$-1/2^-[301]$	$1/2^-[550]$	6.792
$1/2^-[301]$	$3/2^-[541]$	6.134
$-1/2^-[301]$	$1/2^-[541]$	8.383
$-1/2^-[301]$	$1/2^-[530]$	9.980
$-1/2^+[431]$	$1/2^+[431]$	8.734
$-1/2^+[431]$	$1/2^+[420]$	6.797
$1/2^+[431]$	$3/2^+[422]$	6.379
$1/2^+[431]$	$3/2^+[411]$	5.709
$-1/2^+[431]$	$1/2^+[411]$	6.947
$7/2^+[413]$	$9/2^+[404]$	5.373

$7/2^+[413]$	$5/2^+[413]$	5.679
$7/2^+[413]$	$5/2^+[402]$	7.669
$-1/2^+[420]$	$1/2^+[420]$	4.859
$1/2^+[420]$	$3/2^+[422]$	4.442
$1/2^+[420]$	$3/2^+[411]$	3.771
$-1/2^+[420]$	$1/2^+[411]$	5.009
$-1/2^-[550]$	$1/2^-[550]$	4.086
$1/2^-[550]$	$3/2^-[541]$	3.428
$-1/2^-[550]$	$1/2^-[541]$	5.677
$-1/2^-[550]$	$1/2^-[530]$	7.274
$3/2^+[422]$	$5/2^+[413]$	3.878
$3/2^+[422]$	$1/2^+[411]$	4.592
$3/2^+[422]$	$5/2^+[402]$	5.868
$9/2^+[404]$	$7/2^+[404]$	6.300
$3/2^-[541]$	$5/2^-[532]$	2.899
$3/2^-[541]$	$1/2^-[541]$	5.019
$3/2^-[541]$	$1/2^-[530]$	6.616
$3/2^+[411]$	$5/2^+[413]$	3.207
$3/2^+[411]$	$1/2^+[411]$	3.922
$3/2^+[411]$	$5/2^+[402]$	5.197
$5/2^-[532]$	$7/2^-[523]$	4.674
$5/2^+[413]$	$7/2^+[404]$	6.607
$7/2^-[523]$	$9/2^-[514]$	8.541

Table 3: TDA calculations for neutrons structure in ^{102}Mo. X is the amplitude of each couple of orbitals. Each couple is identified by the excitation energy $E_v + E_{v'}$ and the quadrupole moment of mass. $F_{vv'}$ and $G_{vv'}$ are the quadrupole coefficients

<v/ /v'>		$E_v + E_{v'}$	$<v/r^2Y_{22}/v'>$	$F_{vv'}$	$G_{vv'}$	X
$3/2^+[422]$	$1/2^+[431]$	6.379	-0.122	0.438	-0.899	0.010
$3/2^+[422]$	$1/2^+[420]$	4.442	0.952	0.540	-0.841	-0.142
$3/2^+[422]$	$1/2^+[411]$	4.592	-0.141	0.997	0.076	0.037
$3/2^-[541]$	$1/2^-[301]$	6.134	-0.003	0.598	-0.801	-0.001
$3/2^-[541]$	$1/2^-[550]$	3.428	-0.703	0.735	-0.678	-0.189
$3/2^-[541]$	$1/2^-[541]$	5.019	0.589	0.939	0.342	0.134
$3/2^-[541]$	$1/2^-[530]$	6.616	-0.149	0.921	0.390	-0.025
$3/2^+[411]$	$1/2^+[431]$	5.709	0.249	0.919	-0.395	-0.049
$3/2^+[411]$	$1/2^+[420]$	3.771	-0.039	0.959	-0.284	0.012
$3/2^+[411]$	$1/2^+[411]$	3.922	1.328	0.705	0.709	-0.296
$5/2^+[422]$	$1/2^+[431]$	10.327	0.387	0.236	-0.972	0.010
$5/2^+[422]$	$1/2^+[420]$	8.389	-0.855	0.348	-0.937	-0.042
$5/2^+[422]$	$1/2^+[411]$	8.539	0.069	0.990	-0.138	0.009
$5/2^-[303]$	$1/2^-[301]$	9.521	-1.195	0.249	-0.968	-0.037
$5/2^-[303]$	$1/2^-[550]$	6.815	0.001	0.422	-0.906	0.000
$5/2^-[303]$	$1/2^-[541]$	8.406	0.013	0.999	-0.041	0.002
$5/2^-[303]$	$1/2^-[530]$	10.003	0.012	0.999	0.011	0.001
$7/2^+[413]$	$3/2^+[422]$	5.827	0.366	0.456	-0.889	0.035
$7/2^+[413]$	$3/2^+[411]$	5.156	-1.115	0.927	-0.376	-0.244
$9/2^+[404]$	$5/2^+[422]$	7.518	-0.225	0.509	-0.861	-0.018
$9/2^+[404]$	$5/2^+[413]$	3.424	0.269	0.996	0.088	0.098
$9/2^+[404]$	$5/2^+[402]$	5.414	-1.359	0.962	0.273	-0.293
$5/2^-[532]$	$1/2^-[301]$	6.263	-0.003	0.948	-0.319	-0.001
$5/2^-[532]$	$1/2^-[550]$	3.557	-0.612	0.990	-0.140	-0.213
$5/2^-[532]$	$1/2^-[541]$	5.148	0.388	0.579	0.815	0.053
$5/2^-[532]$	$1/2^-[530]$	6.745	-0.825	0.536	0.844	-0.079
$5/2^+[413]$	$1/2^+[431]$	6.232	-0.261	0.978	-0.206	-0.049
$5/2^+[413]$	$1/2^+[420]$	4.2945	-0.003	0.996	-0.089	-0.009
$5/2^+[413]$	$1/2^+[411]$	4.445	-1.177	0.552	0.834	-0.179
$7/2^-[523]$	$3/2^-[541]$	4.545	-0.518	0.948	0.317	-0.132

5/2$^+$[402]	1/2$^+$[431]	8.222	0.023	0.999	-0.019	0.003
5/2$^+$[402]	1/2$^+$[420]	6.285	-0.183	0.995	0.099	-0.035
5/2$^+$[402]	1/2$^+$[411]	6.435	0.073	0.386	0.923	0.005
7/2$^+$[404]	3/2$^+$[422]	6.754	-0.187	0.982	0.188	-0.033
7/2$^+$[404]	3/2$^+$[411]	6.083	-0.012	0.621	0.784	-0.002
9/2$^-$[514]	5/2$^-$[303]	10.154	-0.008	0.999	0.014	-0.001
9/2$^-$[514]	5/2$^-$[532]	6.896	-0.396	0.533	0.846	-0.037

The combinations between states (columns 1 and 2) are treated in the approximation of quasiparticle independent model, where the Hamiltonian is: $H = U_0 + \sum_{\mu\nu}(E_\mu + E_\nu)\alpha^+_\mu\alpha_\nu$, and the correspondent energy is presented in column 3. We find out three possible combinations of states. With smallest energy (E_μ + E_ν) according to the Fermi level, the ground state could be formed from the couple (3/2$^-$[541], 5/2$^-$[532]) with energy level of 2.899 MeV, the couple (1/2$^-$[550], 3/2$^-$[541]) with 3.428 MeV, or the couple (1/2$^+$[420], 3/2$^+$[411]) with 3.771 MeV. Therefore, when comparing these eigen-values with the ones from table 1, we could expect one of the 5/2$^-$[532], 3/2$^-$[541] and 3/2$^+$[411] orbitals to be the ground state of ^{103}Mo. However, in the Tamm-Dancoff Approximation (TDA), the ^{103}Mo could be treated in simple way as a two-body interaction where the shape softness of ^{102}Mo could be introduced in dynamic manner by γ vibration (see equation 24). In table 3, the amplitude values $(X_\gamma)_{\mu\nu}$ of TDA phonon are illustrated for different states combinations around the Fermi level.

As we can note from table 3, the state 3/2$^+$(411) presents the largest vibration -0.296 compared to the nearest ones, -0.213 and -0.189 for 5/2-(532) and 3/2-(541) respectively. Consequently, in the approximation of quasiparticle – phonon coupling model, we adopted the 3/2$^+$[411] orbital, originating from the $\nu g_{7/2}$ subshell, to be the ground state of ^{103}Mo, which is in good agreement with the experimental assignment from [6, 22].

We have shown in figure 2, the comparison between theoretical and experimental energy levels of the collective bands of ^{103}Mo is investigated by our QPRM calculations, in respect to the deformation parameters given by Möller [5], and compared to the existing experimental data [8]. The states characterized by the same asymptotic quantum numbers Ω^π [N, n_z, Λ], where Ω is the quantum number that corresponds to the third component of the angular momentum in the intrinsic frame, π and N being its parity and the principal quantum number of the major oscillator shell, n_z is the number of quanta associated with the wave function moving along the z-direction and Λ is the projection of the orbital angular momentum onto the z axis (symmetry axis). We note that the odd-neutron wave function for the Ω^π = 5/2$^-$ isomer is calculated to have the following asymptotic Nilsson components:

|5/2$^-$> = -0.064[503]+ 0.273 [512]- 0.395 [523]+ 0.875 [532], while that of the Ω^π = 3/2$^+$ ground state has components:

|3/2$^+$> = -0.174[402]+ 0.894[411]- 0.398[422]- 0.106000 [431].

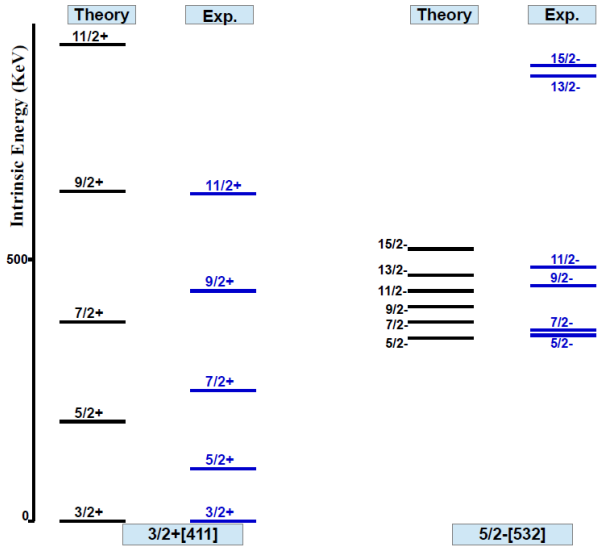

Fig.2: Comparison between experimental and theoretical values of the ground and rotational band for ^{103}Mo using QPRM Method

Through analyzing the intrinsic structure of positive and negative parity side bands, we conclude that the low-excitation deformation bands are attributed to the high-j intruder states $1g_{7/2}$ and $1h_{11/2}$ in the N = 4 , 5 shells. In addition, we conclude from the discussion of quasi-particle bands that the quasi-particles in the orbit ν3/2$^+$[411] and ν5/2$^-$[532] play an important role in the deformation of ^{103}Mo. The ground state found in our calculations is assigned to be 3/2$^+$[411] raising up from $\nu g_{7/2}$, which is in good agreement with the experimental assignment. As discussed in Refs [6, 22], ^{103}Mo has an excited state at 346.6 keV assigned to be 5/2$^-$[532]. Looking at the result of our calculations, this state localized at 349.0 keV, is well predicted to be originating from $\nu h_{11/2}$ orbital. They had been arranged in two structures: the first one, built on the ground state, extends up to spin 11/2$^+$ and the other, with negative parity, extends from spin 5/2$^-$ at 346.6 keV up to spin 15/2$^-$.

Conclusion

We have presented theoretical calculations of intrinsic method based on the quasiparticle-phonon coupling, inspired by MQPM of Soloviev. We used phonon TDA to simplify the calculations with BCS vacuum which is a

phonon TDA vacuum. We have shown that the residual interaction coming from rotational Hamiltonian favours the positive parity states, because of deformation alignment of the states coming from $vh_{11/2}$ spherical orbital. It gives a microscopic description of the structure of transitional nuclei by showing coexistence and contribution of different excitation modes: individual, vibrational and rotational. To obtain intrinsic states, we have used a deformed average field of Nilsson, a monopole pairing and a quadrupole-quadrupole interaction. The states of rotational bands are determined by inclusion of both recoil and Coriolis effects coming from the treatment of the axially symmetric rotational motion. The contribution of vibrational excitation is considered by using the Tamm-Dancoff Approximation (TDA) so as to give a microscopic structure to the bandhead or the phonon state. The quadrupole force tends to deform the nucleus (γ-softness) in such a situation where the spherical shape is stabilized by the pairing force. When more nucleons are added to the spherical shape (closed shell), the relative strength of the quadrupole force increases and at a certain point the transition to the deformed shape takes place.

We have shown for ^{103}Mo that the contribution of quasiparticle-phonon coupling is more important for positive parity states than negative parity ones. At low-spin the excited stated have been obtained by including the Coriolis mixing force. The calculations of negative parity rotational structure built upon the intrinsic state 5/2-[532] have been revised by neglecting the recoil force. Using this quasiparticle-phonon coupling method, we have analysed the low-lying excited levels in ^{103}Mo. In general, the results obtained for ^{103}Mo are in agreement with the experimental data.

References

[1] W. Urban, J.L. Durell, A.G. Smith, W. R.Phillips, M.A. Jones, B.J. Varley, T. Rzaça-Urban, I.Ahmad, L.R. Morss, M. Bentaleb, N. Schulz Nucl. Phys.A 689, 605 (2001).
[2] J. A. Pinston, W. urban, Ch. Droste, J. Genevey,T. Rzaca-Urban (Phys. Rev. C 74, 064304 (2006)).
[3] G. Georgiev et al, CERN- INTC- 2009- 019/ INTC- P- 266 (2009).
[4] H.B. Ding et al, Physical Review C74,054301 (2006).
[5] R. Orlandi et al, Physical Review C73, 054310 (2006).
[6] H. Hua et al Physical Review C 69,014317 (2004).
[7] V.G. Soloviev, Theory of Complex Nuclei, Pergamon Press, Oxford, England, 1976.
[8] O. Jdair, J. Inchaouh, M. K. Jammari, H. Chakir, Vol.3.N°2.March, 2011, Part IV (International Journal of Academic Research).
[9] J.Inchaouh , K.Jammari, O.Jdair, A. Khouaja, M.L.Bouhssa, H. Chakir and A. Morsad. Physical Review C 2013; 88: 064301(12).
[10] P. Ring et P. Schuck, the nuclear Many-body Problem (Springer, New York 1980).
[11] A. Bohr and B. R. Mottelson, Nuclear Structure Vol. 2, Benjamin (1975).
[12] J. M. Eisenberg and W. Greiner; Nuclear Models, Vol. 1 (Elsevier, New York, 1970).
[13] J. P. Boisson and R. Piepenbring, Nucl. Phys. A168 (1971) 385.
[14] W. Ogle, S. Wahlborn, R. Piepenbring et S. Fredriksson, Rev. of Mod. Phys. 43 (1971) 424.
[15] P. Möller et al, Atomic data and Nuclear Data tables, Vol.59, N°. 2 (1995)185.
[16] R. A. Meyer et al Nucl. Phys. A439, 510 (1985).
[17] P. Möller, J. R. Nix, Nucl. Phys. A536 (1992)20.
[18] A. Guessous et al Physical Review C53, 1191 (1996).
[19] L. Grodzins, Phys.Lett.2 (1962) 88.
[20] F.S.Stephens et al, Phys. Rev. Lett.29 (1972) 438.
[21] C. M. Petrache, Y. Sun, D. Buzzacco, S. Lunardi, C. Rossi Alvarez, R. Venturelli, D. De Acuña, G. Maron, M. N. Rao, Z. Podolyak, at J. R. B. Oliveira ; Phys. Rev. C53 (1996) R2581.
[22] D. De Frenne, Nucl. Data Sheets 110, 2081 (2009).